# Threshold detection of continuous phase-modulated signals

K.R. Raveendra, PhD
R. Srinivasan, PhD

*Indexing terms: Signal processing, Noise and interference, Digital communications systems*

**Abstract:** Threshold detection techniques are employed to obtain canonical multiple-bit-observation receivers for detection of weak coherent and incoherent continuous phase-modulated signals buried in non-Gaussian noise. The limiting performance estimates of these receivers are derived, and then used to determine optimum coherent and incoherent threshold signalling schemes that belong to a subclass of CPM signals and find applications over certain bandlimited channels.

## 1 Introduction

Digital transmission using continuous phase-modulated (CPM) signals is an important signalling technique, having widespread applications in mobile communications, terrestrial digital radio and satellite communications. Spectral and power-saving properties of CPM are well known, as are demodulation techniques in Gaussian interference [1–9]. We study here a subclass of CPM known as multi-$h$ CPM [9], which includes multi-$h$ CPFSK and multi-$h$ CPFSK type of signalling with input data pulse shaping [1]. These are energy-efficient signalling techniques with attractive narrow-band spectra.

Over several channels where CPM is employed, signal fading is a major problem, accompanied by difficulties in maintaining phase synchronisation. Furthermore, the weak or threshold signal condition is one that is frequently encountered. This could be caused by the requirement of modern communication systems for the transmitted signal energy to be minimised, for privacy and power economy. Although the performance of CPM signals in Gaussian noise is well studied, not much work [10] has been reported on their performance in noise subject to terrestrial disturbances which are artificial or atmospheric. In fact, in the spectrum below 100 MHz, such disturbances are quite non-Gaussian in character [11–13].

The object of this paper is to consider the general problem of threshold detection of CPM signals in noise subject to terrestrial disturbances that are non-Gaussian in character.

Paper 6920I (E16, E8), first received 23rd February 1988 and in revised form 31st July 1989

Dr. Raveendra is with the Department of Electronics & Communication Engineering, Delhi Institute of Technology, Old I.G. Block, Kashmere Gate, Delhi 110 006, India.

Dr. Srinivasan is with the Department of Electrical & Computer Engineering, Syracuse University, New York 13244, USA.

## 2 CPM signal models

The CPM signal over an $n$-bit interval may be written as

$$s(t, \tilde{a}) = \sqrt{(2S)} \cos(2\pi f_c t + \phi(t, \tilde{a}) + \phi_0) 0 \leqslant t \leqslant nT \quad (1)$$

where $S$ is the power of the signal in the bit duration $T$, $f_c$ is the carrier frequency and $\phi_0$ is the starting phase, which, without loss of generality, may be set equal to zero for coherent transmission. The information-carrying phase in eqn. 1 for multi-$h$ CPM signals can be written as

$$\phi(t, \tilde{a}) = \int_0^t \sum_{i=1}^{n} 2\pi h_i a_i g(\tau - (i-1)T)\, d\tau \quad 0 \leqslant t \leqslant nT \quad (2)$$

where $\tilde{a} = (a_1, a_2, \ldots, a_n)$ is an $n$-bit uncorrelated equally likely binary sequence. Defining the base-band phase function $q(t)$ through the relation

$$q(t) = \int_0^t g(\tau)\, d\tau \quad 0 \leqslant t \leqslant nT \quad (3)$$

eqn. 2 can be written as

$$\phi(t, \tilde{a}) = 2\pi \sum_{i=1}^{n} a_i h_i q(t - (i-1)T) \quad 0 \leqslant t \leqslant nT \quad (4)$$

Among the several phase functions that are commonly employed, we consider the following:

$$q(t) = \begin{cases} 0, & t \leqslant 0,\ t > T;\ \text{REC, HCS, RC} \\ t/2T, & 0 \leqslant t \leqslant T;\ \text{REC} \\ \frac{1}{4}(1 - \cos \pi t/T) & 0 \leqslant t \leqslant T;\ \text{HCS} \\ \frac{1}{2}(t/T - \frac{1}{2\pi} \sin 2\pi t/T) & 0 \leqslant t \leqslant T;\ \text{RC} \\ \frac{1}{2}, & t \geqslant T;\ \text{REC, HCS, RC} \end{cases} \quad (5)$$

Using eqn. 5 in eqn. 4, the excess phase containing the information bits during the $i$th bit interval can be written as

$$\phi(t, \tilde{a}) = 2\pi a_i h_i q(t - (i-1)T) + \pi \sum_{r=1}^{i-1} a_r h_r \quad (i-1)T \leqslant t \leqslant iT \quad (6)$$

The second term in eqn. 6 is the accumulated phase caused by the data bits through $a_{i-1}$, while the first term denotes the time-varying incremental phase over the $i$th bit interval. In eqn. 5, REC, HCS, and RC refer to frequency pulses with rectangular, half-cycle sinusoidal and raised-cosine shapings respectively, and $h_i$ in eqn. 6 is the modulation index employed during the $i$th bit interval.

For binary data transmission using CPFSK, a single modulation index $h = 0.72$, which maximises the detection efficiency, is used. The MSK is a special case of CPFSK with $h = 0.5$. In multi-$h$ CPM a set of modulation indices $\{h_i;\ i = 1, 2, \ldots, K\}$ is employed in a cyclic

manner, i.e. $h_i = h_{i+K} = h_{i+2K}, \ldots, i = 1, 2, \ldots, K$, where $K$ denotes the number of different modulation indices. A subclass of multi-$h$ CPM, wherein REC frequency pulse is employed, is considered in Reference 3 and is termed multi-$h$ phase-coded modulation. In this class of modulation, certain restrictions are placed on the possible membership of the set $\{h_i;\ i = 1, 2, \ldots, K\}$ of modulation indices, which ensure a periodic phase trellis and also permit simple maximum-likelihood decoding by means of a Viterbi-algorithm decoder. The multi-$h$ CPFSK is considered in Reference 5. The class of signals described in this Section can be used to represent a wide variety of digital modulations such as FSK, MSK, CPFSK, multi-$h$ CPFSK etc. through appropriate choice of $\{h_i\}$.

## 3 Coherent threshold receiver

The techniques for deriving threshold-receiver structures for various digital-signalling situations are well known [11, 13–16]. In general, the standard procedure is to replace all waveforms over the decision interval with vectors of $M$ samples and form the likelihood ratio. The sampling process is assumed to result in independent and identically distributed (IID) samples of noise over the decision time interval, so that only first-order probability-density functions (PDFs) are required. For the case of threshold signals, then, using the Taylor series expansion in the likelihood ratio and discarding signal terms of degree 2 and higher, the receiver structure is obtained, which consists of a memoryless nonlinearity followed by a linear matched filter (or correlator) receiver (optimum when the interference is Gaussian in character). The transfer characteristic of the nonlinearity is given by $-d/dr[\ln p_N(r)]$, where $p_N(r)$ is the first-order amplitude PDF of the additive interference.

The performance of the coherent threshold receiver for the limiting case of large sample size and vanishingly small signal strength can be determined by the central limit theorem (CLT), by evaluating only the first two central moments of the output of the receiver, which is the decision variable. Such performance estimates in narrowband non-Gaussian noise for coherent PSK, FSK and ASK may be found in References 11 and 17–19.

Although in all the above analyses receivers are required to make independent bit-by-bit decisions, in Reference 10 a threshold receiver that uses multiple-bit observation for detection of CPFSK signals buried in non-Gaussian noise is derived and its limiting performance estimates are obtained. By extending these results, it can be shown that the threshold receiver structure for detecting weak CPM signals buried in additive non-Gaussian noise consists of a zero-memory nonlinearity, $-d/dr\ [\ln p_N(r)]$, followed by the average matched filter (AMF) receiver for CPM, which for its operation requires only two correlators. One of the correlator reference signals is the average of all transmitted signal waveforms of $n$-bit duration, with the first bit datum $a + 1$ and the other average of all transmitted waveforms with the first bit datum $a - 1$. This receiver is shown in Fig. 1 and uses the detection strategy of observing the signal over $n$-bit intervals and producing an estimate of the first bit datum. It is noted that this receiver is canonical, in that the detection algorithm is independent of the kind of noise encountered. Furthermore, when the interference is Gaussian, the receiver is just the AMF receiver, which is shown to be optimum at low values of the signal/noise ratio (SNR) [4]. Following the technique of Reference 10, and with reference to Fig. 1, the limiting performance of the threshold receiver for multi-$h$ CPM signals can be shown to be given by

$$P_e = (1/K)(1/z^{n-1}) \sum_{p=1}^{K} \sum_{j=1}^{2^{n-1}} Q(|\mu_j^p|/\sigma_p) \tag{7}$$

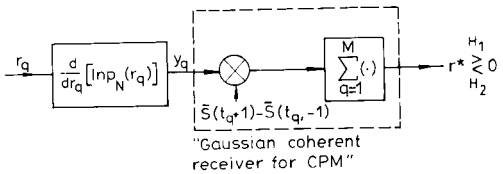


**Fig. 1** *Optimum coherent threshold receiver structure for CPM signals*

where $\mu_j^p$ is the mean of the output decision variable, given a particular data sequence $A_j$ with $a_1 = +1$ transmitted and $\sigma_p^2$ as the variance. The summation $\sum_p$ is used to handle the cyclic variation of $K$ modulation indices employed and $Q(x)$ denotes the area under the zero-mean, unit-variance normal curve from $x$ to infinity.

In Appendix A, the performance analysis of the receiver shown in Fig. 1 is presented and closed-form expressions for $\mu$ and $\sigma$ for signalling schemes described in Section 2 are given.

## 4 Receivers for noncoherent threshold detection

In this Section we derive multiple-bit-observation threshold receiver structures for detecting weak CPM signals subject to slow and fast fadings in non-Gaussian noise. The slow fading refers to the case wherein the amplitude and phase of the received signal are random but constant over the entire decision interval. In the fast-fading case the amplitude and phase are random but constant only over sub-intervals of the decision interval. In both situations, the detection strategy is to observe the received signal over $n$ bit intervals and to produce an estimate of a specific data bit transmitted $a_\delta$, $1 \leqslant \delta \leqslant n$. It is noted that the derivation of the receiver structures is independent of the choice of the decision bit location $\delta$.

### 4.1 Slow-fading case

The detection problem at hand is a composite hypothesis statistical test which may be stated as

$$\left.\begin{aligned} H_1: r(t) &= b\cos(2\pi f_c t \\ &\quad + \phi(t, a_\delta = +1, A_j) + \theta) + n(t) \\ H_2: r(t) &= b\cos(2\pi f_c t \\ &\quad + \phi(t, a_\delta = -1, A_j) + \theta) + n(t) \end{aligned}\right\} \begin{aligned} &0 \leqslant t \leqslant nT \\ &j = 1, 2, \ldots, 2^{n-1} \end{aligned} \tag{8}$$

where $b$ and $\theta$ are composite parameters with the latter uniformly distributed in $(-\pi, +\pi)$ and the former having an arbitrary fading distribution. Further, it is assumed that $b$ and $\theta$ are independent. $A_j$ is the $(n-1)$-tuple $(a_1, \ldots, a_{\delta-1}, a_{\delta+1}, \ldots, a_n)$ and represents another composite parameter whose distribution is easily determined by noting that the data bits are independent and assume values from the set $\{+1, -1\}$. The quantity $\phi(.,.,.)$ in eqn. 8 is the information-carrying phase defined in eqn. 4.

The received waveform in eqn. 8 is uniformly sampled to obtain $M$ samples. Assuming IID noise samples, the composite hypothesis test of optimally deciding between $H_1$ and $H_2$ is given by the likelihood-ratio test (LRT) [20]. Setting up the LRT, making use of the Taylor series expansion for signal level near zero, discarding signal terms of order 3 and higher, and averaging over all com-

posite parameters, it can be shown that the threshold receiver is given via the decision rule

$$\left| \sum_{q=1}^{M} F(r_q)\overline{s_c^p}(t_q, a_\delta = +1) \right|^2 \underset{H_2}{\overset{H_1}{\gtrless}} \times \left| \sum_{q=1}^{M} F(r_q)\overline{s_c^p}(t_q, a_\delta = -1) \right|^2 \quad (9)$$

where

$$F(r_q) = -d/dr_q[\ln p_N(r_q)] \quad (10)$$

and

$$\overline{s_c^p}(t, a_\delta = \pm 1) = \sum_{i=1}^{2^{n-1}} \exp\,[j(2\pi f_c t + \phi(t, a_\delta = \pm 1, A_i))] \quad (11)$$

In eqn. 11, $\overline{s_c^p}(.,.)$ denotes a pair of complex correlator reference signals: one is composed of all transmitted waveforms of $n$-bit duration with $a_\delta = +1$, and the other of all transmitted waveforms with $a_\delta = -1$. The receiver implementing eqn. 9 is shown in Fig. 2, and consists of the noncoherent AMF receiver for CPM preceded by a memoryless nonlinearity $F(r_q)$. The structure of this nonlinearity is precisely the same as that required in the case of coherent threshold receiver. It is noted that the noncoherent AMF receiver for CPM is optimum for low values of the SNR when the additive noise encountered is Gaussian in character [4].

### 4.2 Fast-fading case

The hypothesis testing problem for this case may be stated as

$$\left.\begin{aligned} H_1: r(t) &= \sum_{i=1}^{n} b_i s_i(t, a_\delta \\ &= +1, A_j, \theta_i) + n(t) \\ H_2: r(t) &= \sum_{i=1}^{n} b_i s_i(t, a_\delta \\ &= -1, A_j, \theta_i) + n(t) \end{aligned}\right\} \begin{aligned} &0 \leqslant t \leqslant nT \\ &j = 1, \ldots, 2^{n-1} \end{aligned} \quad (12)$$

where $b_i s_i(.,.,.,.)$ is the signal waveform received during the $i$th bit interval, $b_i$ and $\theta_i$ are the random amplitude and phase of the $i$th bit received signal waveform. These are assumed to be independent of each other. Furthermore, it is assumed that fading is independent from bit to bit. Employing similar steps used for slow-fading case, the decision rule for optimally deciding between $H_1$ and $H_2$ may be shown to be given by

$$\sum_{i=1}^{n} \left| \sum_{q=(i-1)M'+1}^{iM'} F(r_q)\overline{s_{ci}^p}(t_q, a_\delta = +1) \right|^2 \underset{H_2}{\overset{H_1}{\gtrless}} \sum_{i=1}^{n} \left| \sum_{q=(i-1)M'+1}^{iM'} F(r_q)\overline{s_{ci}^p}(t_q, a_\delta = -1) \right|^2 \quad (13)$$

where $M'(=M/n)$ is equal to the number of samples per bit interval, and $\overline{s_{ci}^p}(.,.)$ are the $i$th bit correlator reference signals. The receiver implementing eqn. 13 is shown in Fig. 3.

While the performance analysis of the receiver for the fast-fading case (Fig. 3) appears analytically intractable, closed-form limiting performance estimates of the receiver for the slow-fading case (Fig. 2) may be obtained. This is carried out in the next Section.

## 5 Performance analysis of noncoherent (slow-fading) threshold receiver

In this Section, we use the receiver structure derived in the previous Section to evaluate the performance of the noncoherent receiver for the slow-fading case. To begin with, we suppose hypothesis $H_1$ to be true and a particular data sequence $A_j$ to have been transmitted. Referring to Fig. 2, we observe that $Y_1^p$ and $Y_2^p$ are sums of independent finite-variance random variables and, therefore, are asymptotically complex Gaussian quantities by virtue of the CLT. By making use of the results of Reference 21, it can be shown that the conditional bit error probability

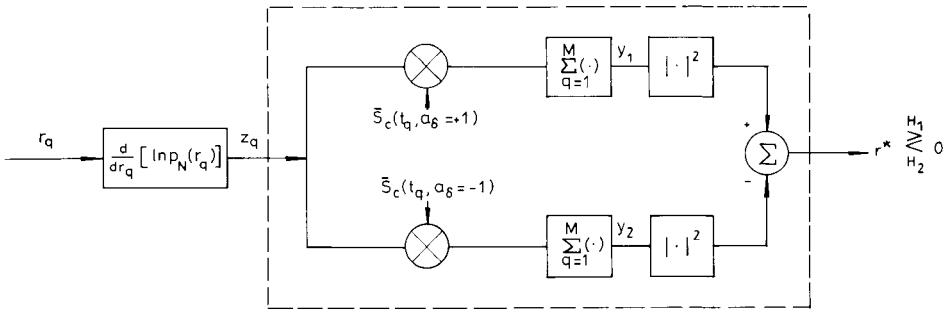


**Fig. 2** *Optimum noncoherent threshold receiver structure for CPM signals (slow-fading case)*

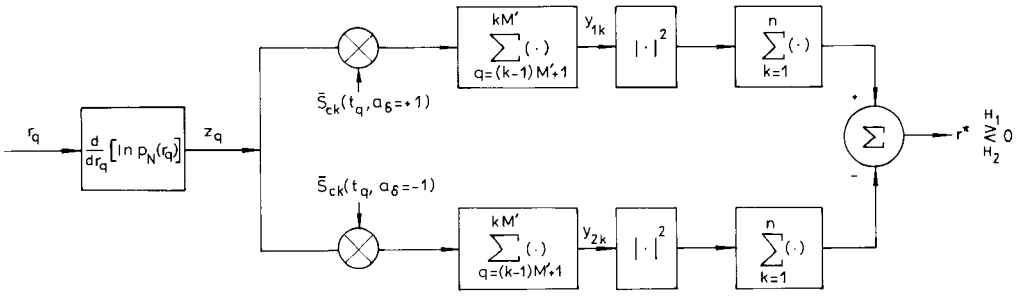


**Fig. 3** *Optimum noncoherent threshold receiver structure for CPM signals (fast-fading case)*

is given by

$$P_{e/H_1, A_j, p} = \text{prob}\,[\,|\,Y_1^p\,|^2 - |\,Y_z^p\,|^2 < 0/H_1, A_j] \qquad (14)$$

which is the probability of one Rician-distributed random variable exceeding another, conditioned on hypothesis $H_1$ and a particular transmitted data sequence $A_j$. The quantity $p$ in eqn. 14 refers to a particular possible arrangement of modulation indices over an $n$-bit decision interval. Averaging eqn. 14 over all possible $A_j$s and sequences of modulation indices, the expression for bit-error probability is given by

$$P_e = (1/K)(1/2^{n-1}) \sum_{p=1}^{K} \sum_{j=1}^{2^{n-1}} P_{e/H_1, A_j, p} \qquad (15)$$

In Appendix B, all steps in arriving at eqn. 15 are given and closed-form expressions for bit-error probability for the signalling schemes described in Section 2 are presented.

## 6 Numerical results and discussion

In obtaining expressions for the performance estimates of the receivers shown in Figs. 1 and 2, no particular noise PDF has been assumed. However, to illustrate the performance of these receivers for detecting weak multi-$h$ CPM signals, we consider the Middleton's class A noise model [11], with its basic parameters given by $A = 0.35$ and $\Gamma' = 0.5 \times 10^{-3}$. The class A noise model has been extensively used in the literature [10, 11, 17], and is often used to model narrow-band artificial noise.

The quantity $L$, given by eqn. 21, denotes the asymptotic relative efficiency (ARE) of the optimum threshold receivers when the noise variance is unity. The ARE represents the performance (for vanishingly small signal strength and very large sample size) of the optimum threshold receiver relative to that of the threshold receiver with $F(r_q) = r_q$ (optimum receiver for Gaussian interference). In fact, the ARE represents the ratio of input sample sizes required by the two receivers operating in the same noise environment to achieve equal probability of error. For the particular Class A noise model we have chosen, to illustrate the performance of threshold receivers, the quantity $L$ has been evaluated [11] with a noise variance of unity and is equal to 1340.

### 6.1 Performance of coherent multi-h CPM

The bit-error probability performance of the coherent threshold receiver may be evaluated using eqn. 7 and the expressions given in Appendix A. The error probability is a function of

(*a*) the sample size $M'$ ($= M/n$)
(*b*) the quantity $L$
(*c*) the SNR $S$
(*d*) the number of observation intervals $n$
(*e*) the set of modulation indices $\{h_i; i = 1, 2, \ldots, K\}$, and
(*f*) the phase function $q(t)$.

For a given phase function $q(t)$, the optimum set $\{h_i; i = 1, 2, \ldots, K\}$ of modulation indices which should be chosen is obviously the one that minimises the bit-error probability of eqn. 7. For a fixed small SNR of $-55$ dB and for a large sample size of $M'$ ($= 1000$), optimum $\{h_i\}$s were determined that minimised the probability of bit error, as a function of number of observation intervals. All three phase functions (REC, HCS and RC) were considered.

The optimum modulation indices, for single-bit observation receivers for REC, HCS and RC systems are 0.72, 0.63 and 0.59, respectively. In Fig. 4 is shown the performance of the optimum single-bit RC system, as a function of SNR and sample size. For $n = 2, 3, \ldots$, for all three phase functions, it is noted that the set $\{h_i = 0.5; i = 1, 2, \ldots, K\}$ minimises the error probability $P_e$. The minimum $P_e$ thus obtained, for all cases, equals the performance of PSK/MSK at $S = -55$ dB and $M' = 1000$. Fig. 5 shows the error probability performance of MSK/PSK. The performances of CPFSK and multi-$h$ CPM

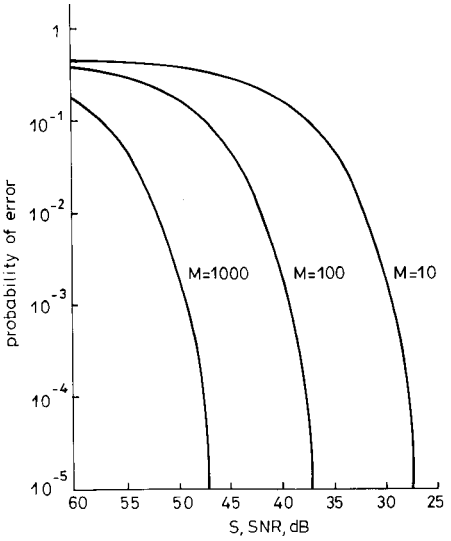


**Fig. 4** *Error-probability performance of optimum coherent threshold receiver for optimum single-bit RC system for Middleton's class A noise model ($A = 0.35$, $\Gamma' = 0.5 \times 10^{-3}$)*
$L = 1340$, $h = 0.72$

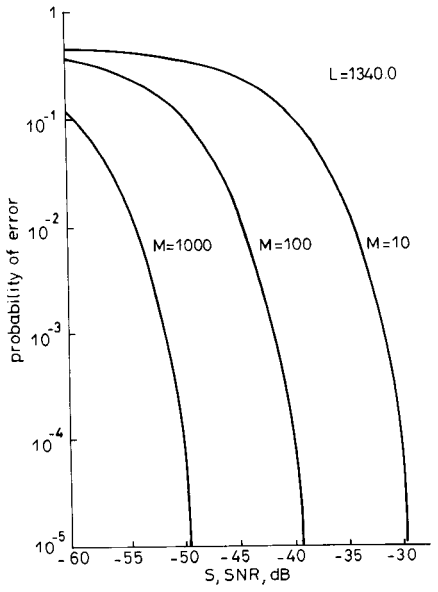


**Fig. 5** *Error probability performance of optimum coherent threshold receiver for MSK for Middleton's class A noise model ($A = 0.35$, $\Gamma' = 0.5 \times 10^{-3}$)*
$L = 1340.0$

(REC) systems are illustrated in Figs. 6 and 7, respectively, as a function of observation interval and sample size.

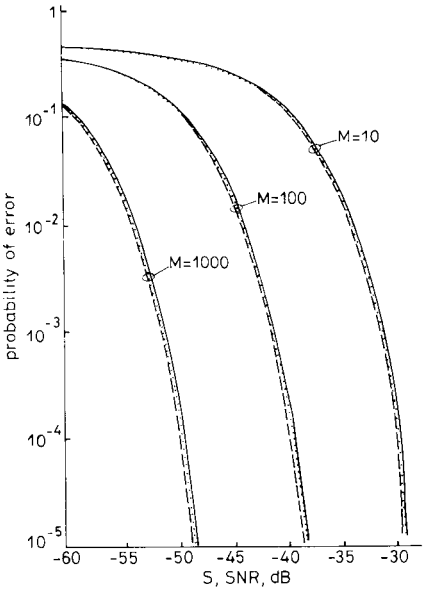


**Fig. 6** *Error-probability performance of optimum threshold receiver for CPFSK, Middleton's class A noise model*
($A = 0.35, \Gamma' = 0.5 \times 10^{-3}$)
– – – – MSK
····· CPFSK $h = 0.715, n = 4$
—— CPFSK $h = 0.715, n = 3$

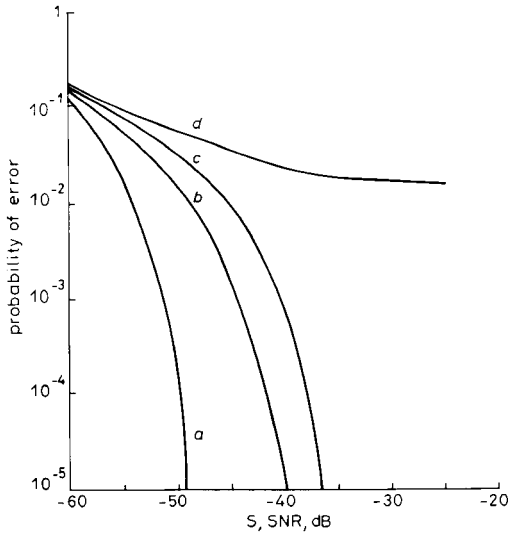


**Fig. 7** *Error-probability performance of optimum threshold receiver for multi-h CPM (REC) systems for Middleton's class A noise model*
*a* $\{\frac{1}{2}, \frac{1}{2}\}; n = 2$
*b* $\{\frac{8}{16}, \frac{5}{16}, \frac{6}{16}, \frac{6}{16}\}; n = 5$
*c* $\{\frac{2}{8}, \frac{3}{8}\}; n = 3$
*d* $\{\frac{8}{15}, \frac{4}{15}, \frac{5}{15}\}; n = 4$

It is well known [6] that CPM offers tradeoffs between power, bandwidth and receiver complexity. To illustrate this ability of weak multi-*h* CPM signals in non-Gaussian noise, in Figs. 8–11 and 12–15 we have

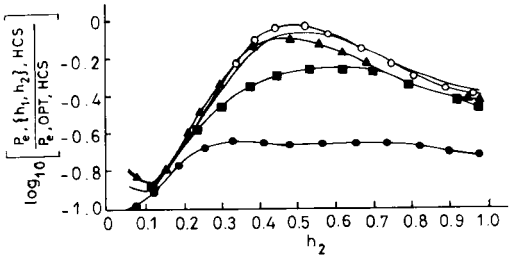


**Fig. 8** *Performance of $\{h_1, h_2\}$ multi-h CPM (REC) ($n = 2$) system relative to MSK in Middleton's class A noise ($A = 0.35, \Gamma' = 0.5 \times 10^{-3}$)*
—●— $h_1 = 0.2$
—▲— $h_1 = 0.4$
—○— $h_1 = 0.5$
—— $h_1 = 0.6$
—■— $h_1 = 0.8$
$L = 1340$, $S = -55$ dB, $M = 1000$, $n = 2$

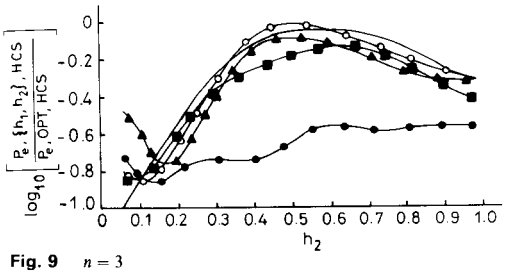


**Fig. 9** $n = 3$

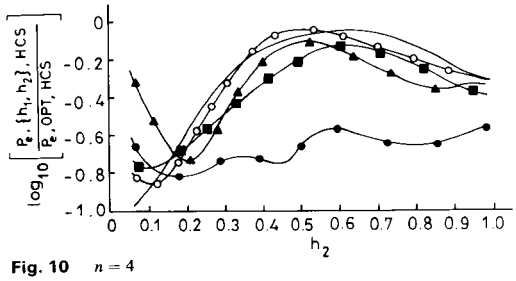


**Fig. 10** $n = 4$

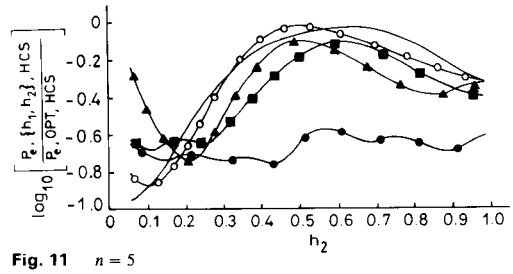


**Fig. 11** $n = 5$

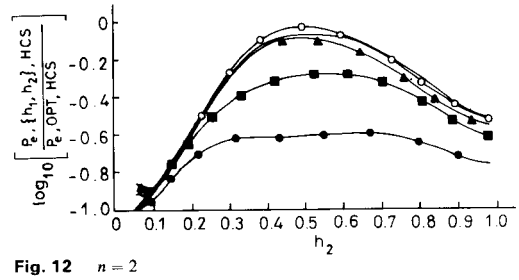


**Fig. 12** $n = 2$

plotted performances of 2-$h$ REC and HCS systems respectively, relative to that of the performance of MSK, which happens to be the optimum threshold multi-$h$

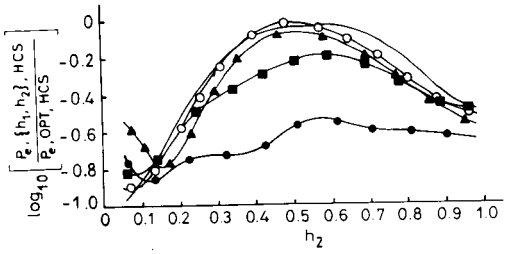


**Fig. 13** $n = 3$

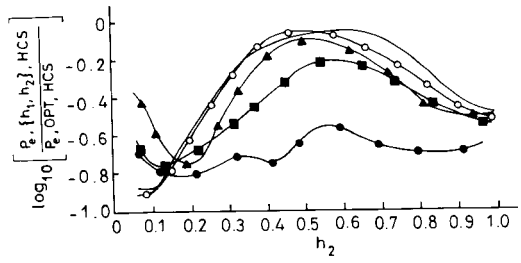


**Fig. 14** $n = 4$

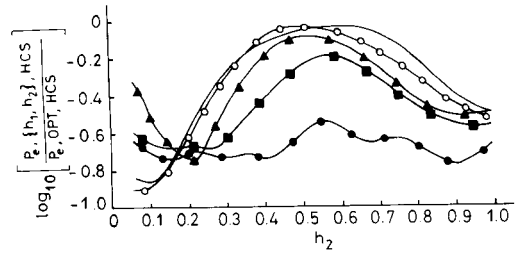


**Fig. 15** $n = 5$

CPM system for all three phase functions considered in this paper. To understand the significance of these plots, let us consider Figs. 8–11, where relative error probabilities of 2-$h$ CPM (REC) and MSK systems are plotted for $n = 2$, 3, 4 and 5, for a fixed SNR of $-55$ dB and sample size $M' = 1000$. Further, let us suppose we have chosen from some system design considerations the set of modulation indices to be $\{0.5, 0.75\}$. Now, for this 2-$h$ CPM system we can determine the optimum observation interval of the threshold receiver by consulting Figs. 8–11, and determining the smallest value of $n$ for which the quantity

$$\log_{10}\left[\frac{P_{e\{0.5,\,0.75\},\,REC}}{P_{e,\,MSK}}\right]$$

is maximum. For the particular case at hand the optimum observation interval is equal to 4 bits, which means that for this observation interval, $\{0.5, 0.75\}$ CPM (REC) system performs closest to the optimum threshold CPM system, which is MSK. It is noted that although $n = 4$ is optimum, by choosing $n = 3$ the loss of performance is only marginal.

### 6.2 Performance of noncoherent multi-h CPM

The error-probability performance of the noncoherent (slow-fading) threshold receiver shown in Fig. 2 for detecting weak multi-$h$ CPM signals in non-Gaussian noise can be determined using eqn. 15 and expressions given in Appendix 10. Clearly, the error probability, as in the coherent case, is a function of $M'$, $L$, $S$, $n$, $\{h_i: i = 1, 2, \ldots, K\}$, $q(t)$ and the decision-bit location $\delta$.

In Fig. 16, the performance of single-bit FSK is shown as a function of sample size. To determine the optimum

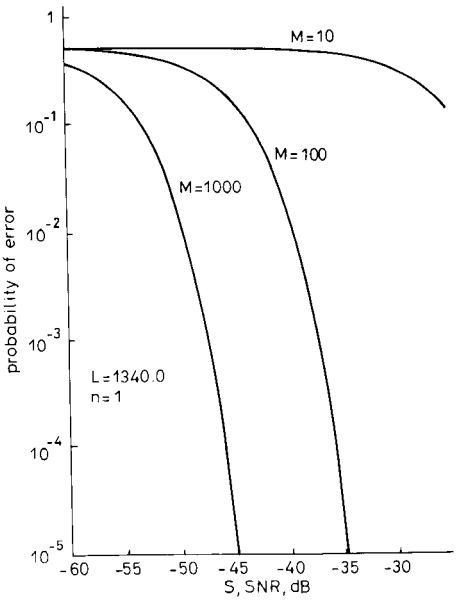


**Fig. 16** *Error-probability performance of optimum noncoherent threshold receiver for FSK for Middleton's class A noise model* ($A = 0.35$, $\Gamma' = 0.5 \times 10^{-3}$)
$L = 1340.0$, $n = 1$

noncoherent threshold signalling schemes, $P_e$, given by eqn. 15, was minimised as a function of $n$ and $\delta$, to arrive at optimum sets $\{h_1, h_2\}$, at a fixed low SNR of $-55$ dB and $M' = 1000$. All three phase functions were considered. It is borne out by our results that the minimum $P_e$ for odd observation intervals is obtained for $\delta = \text{int}\,(n/2) + 1$ and for even observation intervals the decision-bit location $\delta = n/2$ or $n/2 + 1$. It is also observed that for all observation intervals, regardless of the decision-bit location, the set $\{h_1, h_2\}$ that minimises $P_e$ for a given $S$ and $M'$ has the property $h_1 = h_2$; $0 \leqslant h_1$, $h_2 \leqslant 1.0$. This indicates that going for multi-modulation indices in CPM results in no improvement in performance compared to the optimum single-$h$ CPM. In Fig. 17, the performance of the noncoherent threshold receiver for an optimum single $h$ CPM system with REC phase function is shown.

From Fig. 17, it is observed that single-$h$ CPM (REC) system with $h = 0.88$, using a two-bit noncoherent threshold receiver that makes a decision on either of the two bits, can outperform orthogonal FSK. The improvement thus obtained is of the order of 1 dB. The optimum single-$h$ CPM (REC) systems for $n = 3$, 4 and 5 have performance improvements, relative to that of single-bit orthogonal FSK, of 2, 2.25 and 2.5 dB, respectively. The optimum CPM (REC) system for $n = 5$, however, turns out to be inferior to the PSK system by nearly 1.25 dB. It is anticipated that a CPM (REC) system with observation length greater than $5T$ can perform quite close to (within about 0.5 dB) the PSK system. Likewise, observations regarding CPM systems with HCS and RC phase

functions reveal similar performances but with different modulation indices.

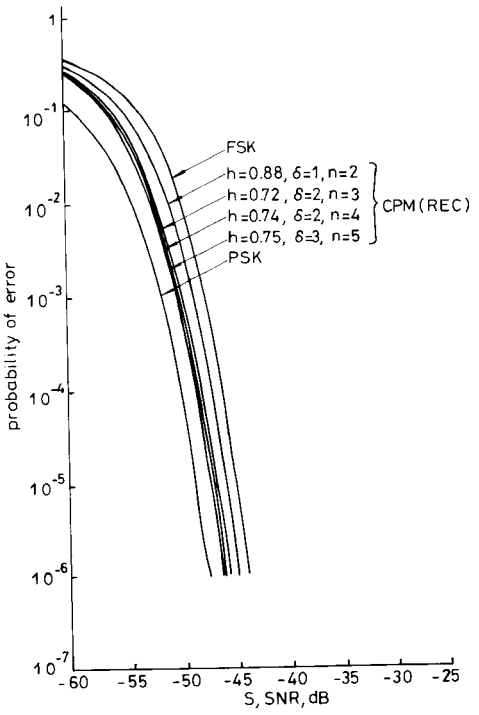


**Fig. 17** *Performance of optimum noncoherent threshold receiver for optimum CPM (REC) systems for class A noise model ($A = 0.35$, $\Gamma = 0.5 \times 10^{-3}$)*

$L = 1340.0$ $M = 1000$

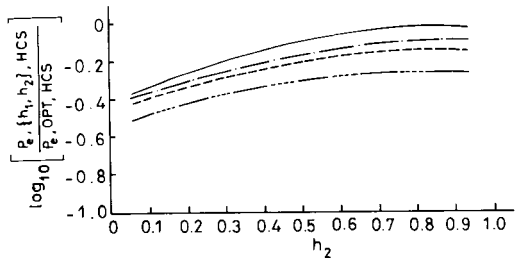


**Fig. 18** *Performance of $\{h_1, h_2\}$ multi-h CPM (REC) system ($n = 2$, $\delta = 1$) relative to optimum CPM (REC) system ($n = 2$, $\delta = 1$) in class A noise ($A = 0.35$, $\Gamma = 0.5 \times 10^{-3}$)*

$L = 1340$, $M = 1000$, $S = -55$ dB, $n = 2$, $\delta = 1$

—— $h_1 = 0.8$

—·— $h_1 = 0.5$

– – – $h_1 = 0.4$

—··— $h_1 = 0.2$

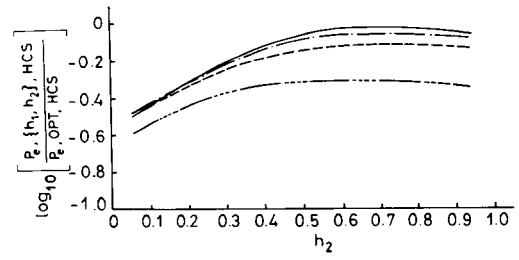


**Fig. 19** $n = 3, \delta = 2$

To understand the tradeoffs inherent in noncoherent multi-$h$ CPM systems, in Figs. 18–21 and 22–25 per-

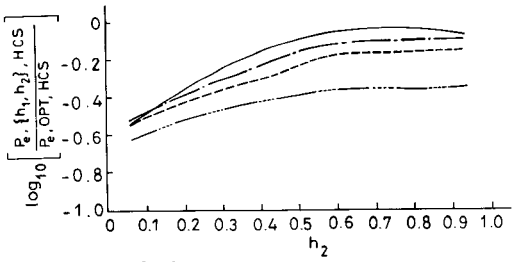


**Fig. 20** $n = 4, \delta = 2$

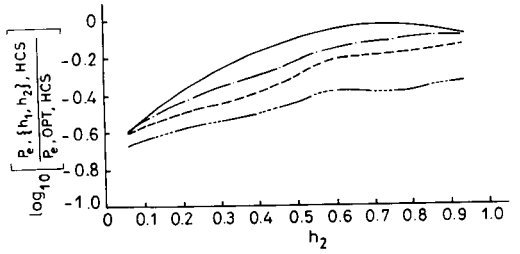


**Fig. 21** $n = 5, \delta = 3$

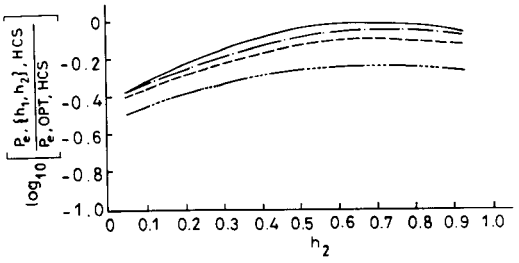


**Fig. 22** $n = 2, \delta = 1$

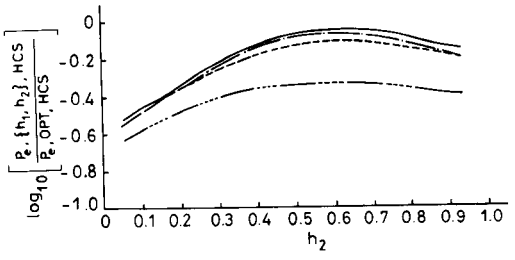


**Fig. 23** $n = 3, \delta = 2$

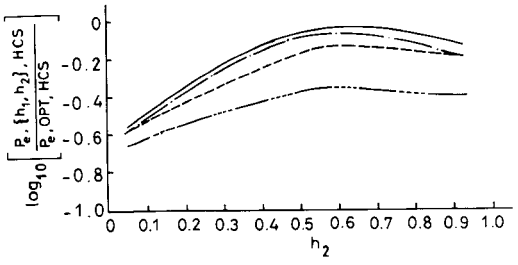


**Fig. 24** $n = 4, \delta = 2$

formances of $\{h_1, h_2\}$ REC and HCS systems have been plotted relative to optimum single-$h$ REC and HCS

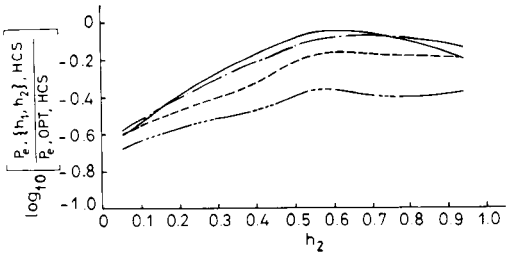


**Fig. 25** $n = 5, \delta = 3$

systems, respectively. In all these plots, optimum decision-bit locations are employed and $S$ is fixed at $-55$ dB and $M'$ at 1000. From plots given in Fig. 20, it is amply clear that there exists a wide range of 2-$h$ CPM (REC) stytems ($\{h_1, h_2\}$; $0.5 \leqslant h_1, h_2 \leqslant 1.0$) that perform close to the optimum $\{h_1, h_2\}$ CPM (REC) system for observation length $4T$. That is, we can choose $\{h_1, h_2\}$ CPM (REC) system, for $n = 4$, that performs close to and is more bandwidth-efficient than the optimum single-$h$ CPM (REC) system. In a similar fashion, the plots of Figs. 22–25 can be used in arriving at optimum $\{h_1, h_2\}$ CPM (HSC) systems relative to optimum single-$h$ systems.

## 7 Conclusions

In this paper, we have considered the problem of coherent and incoherent threshold detection of CPM signals in non-Gaussian noise. Receiver structures have been derived and their performances for detecting multi-$h$ CPM with rectangular, half-cycle sinusoidal and raised-cosine phase functions have been obtained in closed form. For both coherent and incoherent (slow-fading) detection situations, optimum CPM signalling parameters have been determined, and, for the incoherent (fast-fading) case we have arrived at the optimum threshold receiver structure, whose performance analysis appears analytically intractable. Although the use of time-varying modulation indices in CPM seems to offer no further improvement in error-probability performance relative to optimum single-$h$ CPM systems, the former systems for threshold signalling can be designed that are more bandwidth efficient with negligible degradation in performance compared to the latter systems.

## 8 References


1 AULIN, T.: 'Three papers on continuous phase modulation'. PhD dissertation, Telecommunication Theory Dept., University of Lund, Sweden, 1979
2 Special section on 'Modulation and encoding', *IEEE Trans.*, 1981, **COM-29**, pp. 185–297
3 ANDERSON, J.B., and TAYLOR, D.P.: 'A bandwidth-efficient class of signal-space codes', *IEEE Trans.*, 1978, **IT-24**, pp. 703–712
4 OSBORNE, W.P., and LUNTZ, M.B.: 'Coherent and noncoherent detection of CPFSK', *IEEE Trans.*, 1974, **COM-22**, pp. 1023–1036
5 AULIN, T., and SUNDBERG, C.E.: 'On the minimum Euclidean distance for a class of signal space codes', *IEEE Trans.*, 1982, **IT-28**, pp. 43–55
6 HO, P., and MCLANE, P.J.: 'Spectrum, distance, and receiver complexity of encoded continuous phase modulation'. Proc. Global Telecommunications Conference, Atlanta, GA, 1984, pp. 32.3.1–32.3.6
7 PAWULA, R.F., and GOLDEN, R.: 'Simulations and convolutional coding/Viterbi decoding with noncoherent CPFSK', *IEEE Trans.*, 1981, **COM-29**, pp. 1522–1527
8 SVENSSON, A., and SUNDBERG, C.E.: 'On error probability for several types of noncoherent detection of CPM'. Proc. Global Telecommun. Conf., Atlanta, GA, 1984, pp. 22.5.1–22.5.7
9 RAVEENDRA, K.R., and SRINIVASAN, R.: 'Coherent detection of binary multi-$h$ CPM', *Proc. IEE F*, 1987, (4), pp. 416–426
10 RAVEENDRA, K.R., and SRINIVASAN, R.: 'Threshold detection of CPFSK in non-Gaussian noise', *Proc. IEE F*, 1984, **131**, (4), pp. 397–402
11 SPAULDING, A.D., and MIDDLETON, D.: 'Optimum reception in an impulsive interference environment — Parts I and II', *IEEE Trans.*, 1977, **COM-25**, pp. 910–934
12 LEE, W.C.Y.: 'Mobile communications engineering' (McGraw-Hill, 1982)
13 MIDDLETON, D.: 'An introduction to statistical communication theory' (McGraw-Hill, 1960)
14 LU, N.H., and EISENSTEIN, B.A.: 'Detection of weak signals in non-Gaussian noise', *IEEE Trans.*, 1981, **IT-27**, pp. 755–771
15 MILLER, J.H., and THOMAS, J.B.: 'Detectors for discrete-time signals in non-Gaussian noise', *IEEE Trans.*, 1972, **IT-18**, pp. 241–250
16 MODESTINO, J.W., and NINGO, A.Y.: 'Detection of weak signals in narrowband non-Gaussian noise', *IEEE Trans.*, 1979, **IT-25**, pp. 592–600
17 MARAS, A.M., DAVIDSON, H.D., and HOLT, A.G.J.: 'Resolution of binary signals for threshold detection in narrowband non-Gaussian noise', *IEE Proc. F, Commun., Radar & Signal Process.*, 1985, **132**, pp. 187–192
18 BELLOW, P.A., and ESPOSITO, R.: 'The effects of impulsive noise on FSK digital communications', *AEU*, 1973, **27**, pp. 25–29
19 IZZO, L., and PAURA, L.: 'Character error probabilities for $M$-ary CPSK signals subject to Gaussian and impulsive noise', *Alta Freq.*, 1981, **L**, pp. 185–191
20 VAN TREES, H.L.: 'Detection, estimation and modulation theory'. Part I, Sec. 4.4 (Wiley, 1968)
21 SCHWARTZ, M., BENNET, W.R., and STEIN, S.: 'Communication systems and techniques' (McGraw-Hill, 1966)
22 PARL, S.: 'A new method for calculating the generalized Q function', *IEEE Trans.*, 1980, **IT-26**, pp. 121–124


## 9 Appendix A

The $i$th bit correlator reference signals in Fig. 1, for multi-$h$ CPM, may be shown to be given by

$$\bar{s}_i^p(t, a_1 = \pm 1) = \sqrt{(2S)} \cos(2\pi h_{[i]}^{(p)} q(t - (i-1)T) \times \cos(2\pi f_c t \pm \pi h_{[1]}^{(p)}) \beta_p(i) \quad (i-1)T \leqslant t \leqslant iT \quad (16)$$

where $q(t)$ is defined in eqn. 5 for the three phase functions (REC, HCS, RC) considered in this paper. The reference signals during the first bit interval are given by

$$\bar{s}_1^p(t, a_1 = \pm 1) = \sqrt{(2S)} \cos(2\pi f_c t \pm 2\pi h_{[1]}^{(p)} q(t)), \quad 0 \leqslant t \leqslant T \quad (17)$$

Denoting the transmitted signal by $s^p(t, a_1 = +1, A_j)$, the decision variable $r_p^*$ in Fig. 1 may be written as

$$r_p^* \equiv \sum_{i=1}^{M} F(r_i)[s^p(t_i, a_1 = +1) - s^p(t_i, a_1 = -1)] s^p(t, a_1 = +1, A_j) \quad (18)$$

The mean and variance of $r_p^*$ conditioned on hypothesis $H_1$ and $j$th of the $2^{n-1}$ possible data sequences of $(a_2, \ldots, a_n)$, may be shown to be given by

$$\mu_j^p \equiv E\{r_p^*/H_1, A_j\} \simeq -L \sum_{i=1}^{M} \{\bar{s}^p(t_i, a_1 = +1) - \bar{s}^p(t_i, a_1 = -1)\} \times s^p(t_i, a_1 = +1, A_j) \quad (19)$$

$$\sigma_p^2 = \text{var}\{r_p^*/H_1, A_j\} \simeq \sum_{i=1}^{M} \{\bar{s}^p(t_i, a_1 = +1) - \bar{s}^p(t_i, a_1 = -1)\}^2 \times [L - (Ls^p(t_i, a_1 = +1, A_j)^2] \quad (20)$$

where

$$L = \int_{-\infty}^{-\infty} \left[\frac{d}{dr} p_N(r)\right]^2 [p_N(r)]^{-1}\, dr \tag{21}$$

Making use of a small signal approximation, $SL \ll 1$, and for large $M$ approximating the summations in eqns. 19 and 20 by integrals, the mean and variance required in the evaluation of error probability via eqn. 7 are given by

$$\mu_j^p = \mathrm{SLM}'\left\{C_1 + \sin \pi h_{[1]}^{(p)} \sum_{k=2}^{n} \beta_p(k)[\sin \theta_{jk}^{(p)} + C_k]\right\} \tag{22}$$

$$\sigma_p^2 = \mathrm{SLM}'\{2C_1 + (1 - \cos \pi h_{[1]}^{(p)}) \sum \beta_p^2(k) D_k\} \tag{23}$$

where

$$C_1 = \begin{cases} 1 - \mathrm{sinc}\,(2h_{[1]}^{(p)}), \text{ REC} \\ 1 - \cos \pi h_{[1]}^{(p)} J_0(\pi h_{[1]}^{(p)}), \text{ HCS} \\ 1 - P(h_{[1]}^{(p)}), \text{ RC} \end{cases} \tag{24}$$

$$C_k = \begin{cases} (a_k^j/2\pi h_{[k]}^{(p)})[\cos \theta_{jk}^{(p)} - \cos (\theta_{jk}^{(p)} \\ \quad + 2\pi a_k^j h_{[k]}^{(p)})], \text{ REC} \\ J_0(a_k^j \pi h_{[k]}^{(p)}) \sin (a_k^j \pi h_{[k]}^{(p)} + \theta_{jk}^{(p)}), \text{ HCS} \\ \sin (\theta_{jk}^{(p)}) P(a_k^j h_{[k]}^{(p)}) + \cos \theta_{jk}^{(p)} R(a_k^j h_{[k]}^{(p)}), \text{ RC} \end{cases} \tag{25}$$

and

$$D_k = \begin{cases} 1 + \mathrm{sinc}\, 2h_{[k]}^{(p)}, \text{ REC} \\ 1 + \cos (\pi h_{[k]}^{(p)}) J_0(\pi h_{[k]}^{(p)}), \text{ HCS} \\ 1 + P(h_{[k]}^{(p)}), \text{ RC} \end{cases} \tag{26}$$

In eqns. 22–26,

$$\theta_{jk}^{(p)} = \pi \sum_{r=1}^{k-1} a_r^j h_{[r]}^{(p)} \tag{27}$$

$$\beta_p(k) = \prod_{i=1}^{K} \cos^{\alpha_i(k)} \pi h_{[i]}^{(p)} \tag{28}$$

$$J_0(x) = 1/\pi \int_0^{\pi} \cos (x \cos \theta)\, d\theta \tag{29}$$

$$P(x) = 1/2\pi \int_0^{2\pi} \cos (xy - x \sin y)\, dy \tag{30}$$

and

$$R(x) = 1/2\pi \int_0^{2\pi} \sin (xy - x \sin y)\, dy \tag{31}$$

The quantity $\alpha_i(.)$ is given in Table 1 of Reference 10.

## 10 Appendix B

In obtaining the complex correlator references required in the receiver shown in Fig. 2, we assume, for convenience, that all possible waveforms have zero excess phase at the beginning of the decision-bit interval and that $t = 0$ corresponds to the beginning of this interval. Then, the reference signals for multi-$h$ CPM during the decision bit $\delta$ are given by

$$\overline{s_c^p}(t, a_\delta = \pm 1) = \exp\,[j(2\pi f_c t \pm 2\pi h_{\pm[1]}^{(p)} q(t))] \qquad 0 \leqslant t \leqslant T \tag{32}$$

The complex reference signals during the $i$th bit interval after and before the decision bit interval are given by

$$\overline{s_c^p}(t, a_\delta = \pm 1) = \begin{cases} \bar{\prod_k} \cos (2\pi h_{-[k]}^{(p)} q(t)) e^{j2\pi f_c t} \\ \quad 1 \leqslant k \leqslant n_1;\ (k-1)T \leqslant t \leqslant kT \\ \overset{+}{\prod_k} \cos (2\pi h_{+[k+1]}^{(p)} q(t - kT)) e^{j(2\pi f_c t + \pi h_{+[1]}^{(p)})} \\ \quad 1 \leqslant k \leqslant n_2;\ kT \leqslant t \leqslant (k+1)T \end{cases} \tag{33}$$

where

$$\bar{\prod_k} = \prod_{i=1}^{K} \cos^{\gamma_i(k)} \pi h_{[i]}^{(p)} \tag{34}$$

and

$$\overset{+}{\prod_k} = \prod_{i=1}^{K} \cos^{\alpha_i(p)} \pi h_{+[i]}^{(p)} \tag{35}$$

The quantities $\alpha_i(.)$ in eqn. 35 are as given by Table 1 of Reference 10 and $\gamma_i(.)$ in eqn. 34 is given by Table 1 of this Appendix. $n_1$ denotes the number of bits observed before the decision bit interval and $n_2$ after the decision bit interval.

**Table 1: Values of $\gamma_i(k)$ ($k = 1, 2, \ldots$; $m = 0, 1, \ldots$)**

| $k$ | $\gamma_1(k)$ | $\gamma_2(k)$ | $\gamma_3(k)$ | $\cdots$ | $\gamma_K(k)$ |
|---|---|---|---|---|---|
| $mK+1$ | $m$ | $m$ | $m$ | $\cdots$ | $m$ |
| $mK+2$ | $m+1$ | $m$ | $m$ | $\cdots$ | $m$ |
| $mK+3$ | $m+1$ | $m+1$ | $m$ | $\cdots$ | $m$ |
| $\vdots$ | $\vdots$ | $\vdots$ | $\vdots$ | | $\vdots$ |
| $mK+K$ | $m+1$ | $m+1$ | $m+1$ | $\cdots$ | $m$ |

For the sake of convenience, we represent the sequence of modulation indices employed over the $n$ bit intervals by

$$(h_i)^p = (h_{[n_1]}^{(p)}, \underline{h}_{[n_1-1]}^{(p)}, \ldots, \underline{h}_{-[1]}^{(p)}, \boldsymbol{h}_{+[1]}^{(p)}, \ldots, h_{+[n_2+1]}^{(p)}) \tag{36}$$

It can easily be seen that the various possible arrangements of modulation indices over the $n$ observation intervals can be written as

$$\begin{aligned} (h_i)^1 &= (\ldots, h_{k-1}, h_k, \boldsymbol{h}_1, h_2, \ldots, h_K, h_1, \ldots) \\ (h_i)^2 &= (\ldots, h_K, h_1, \boldsymbol{h}_2, h_3, \ldots, h_K, h_1, \ldots) \\ &\vdots \\ (h_i)^k &= (\ldots, h_{K-2}, h_{k-1}, \boldsymbol{h}_K, h_1, \ldots, h_K, h_1, \ldots) \end{aligned} \tag{37}$$

In eqns. 36 and 37, the modulation indices indicated in bold refer to the ones used during the decision bit interval, and $p$ refers to the suffix of the modulation index employed during this interval.

The performance of the receiver shown in Fig. 2 may be evaluated by conditioning on $H_1$ and $A_j$, and assuming that a particular sequence of modulation indices is employed over $n$-bit intervals, say $p$. The received $i$th sample is then given by

$$r(t_i) = \sqrt{(2S)} \cos\,[2\pi f_c t_i + \phi^{(p)}(t_i, a_\delta = +1, A_j) + \theta] + n(t_i) \quad 1 \leqslant i \leqslant M;\ 0 \leqslant t_i \leqslant nT \tag{38}$$

Because, in the receiver, summation and squaring operations are involved, the random phase $\theta$ is set equal to zero and performance analysis is carried out. By noting the transformation on the input sample given by eqn. 10, the first two moments of the $i$th sample at the output of the nonlinearity are given by

$$E\{z_{i/H_1, A_j}^p\} = -L\sqrt{(2S)} \cos\,(2\pi f_c t_i + \phi^{(p)}(t_i, a_\delta = +1, A_j)) \tag{39}$$

and

$$E\{z_{i/H_1, A_j}^2\} = L \tag{40}$$

where $L$ is given by eqn. 21. With reference to Fig. 2, $Y_1$ and $Y_2$ for a particular sequence of modulation indices, say $p$, in terms of the received samples $z_i$, can be expressed as

$$Y^p_{l/H_1, A_j} = \sum_{i=1}^{M} z^p_{i/H_1, A_j} \overline{s^p_c}(t_i, a_\delta = \pm 1)$$
$$l = 1 \text{ for } a_\delta = +1;\ l = 2 \text{ for } a_\delta = -1 \quad (41)$$

By noting the action of the nonlinearity on the received samples in eqn. 41, and making use of the CLT, it is easily observed that $Y^p_l$ are complex Gaussian random variables. By making use of Reference 21, the conditional probability of an error is given by

$$\text{prob}\,[\,|Y^p_1|^2 - |Y^p_2|^2 < 0/H_1, A_j] = 1/2[1 - Q_M(\sqrt{y}, \sqrt{x}) + Q_M(\sqrt{x}, \sqrt{y})] \quad (42)$$

where

$$\left\{\begin{matrix} y \\ x \end{matrix}\right\} = \frac{1}{2\sigma_p^2}\left[\frac{|\mu^p_{1j}|^2 + |\mu^p_{2j}|^2 - 2\,\text{Re}\,(\mu^p_{1j}\mu^p_{2j}\rho^p)}{1 - |\rho^p|^2} \pm \frac{|\mu^p_{1j}|^2 - |\mu^p_{2j}|^2}{\sqrt{1 - |\rho^p|^2}}\right] \quad (43)$$

where $Q_M(.,.)$ is the Marcum-$Q$ function [22]. The various quantities in eqn. 43 can be shown to be given by

$$\mu^p_{1j} \simeq L\sqrt{2S}\sum_{i=1}^{M} \cos\,(2\pi f_c t_i + \phi^{(p)}(t_i, a_\delta = +1, A_j)) \times \overline{s^p_c}(t_i, a_\delta = +1) \quad (44)$$

$$\mu^p_{2j} \simeq L\sqrt{2S}\sum_{i=1}^{M} \cos\,(2\pi f_c t_i + \phi^{(p)}(t_i, a_\delta = +1, A_j)) \times \overline{s^p_c}(t_i, a_\delta = -1) \quad (45)$$

$$\sigma_p^2 \simeq L\sum_{i=1}^{M} |\overline{s^p_c}(t_i, a_\delta = \pm 1)|^2 \quad (46)$$

and

$$\rho^p\sigma_p^2 \simeq L\sum_{i=1}^{M} \overline{s^p_c}^*(t_i, a_\delta = +1) s^p_c(t_i, a_\delta = -1) \quad (47)$$

where * denotes the complex conjugate. In arriving at eqns. 46 and 47, we have made use of the small-signal approximation $SL \ll 1$. For large values of $M$, approximating the summations in eqns. 44–47 by integrals and using suffixes $-1$, 0, $+1$ to denote contributions from before, during and after the decision bit interval in these integrals, for multi-$h$ CPM signals we obtain the following expressions:

$$\mu^p_{1j} = (LM'/2)\sqrt{(2S)}(A_{-1} + A_0 + A_{+1}) \quad (48)$$

$$\mu^p_{2j} = (LM'/2)\sqrt{(2S)}(B_{-1} + B_0 + B_{+1}) \quad (49)$$

$$\sigma_p^2 = LM'(V_{-1} + V_0 + V_{+1}) \quad (50)$$

$$\rho^p\sigma_p^2 = LM'(R_{-1} + R_0 + R_{+1}) \quad (51)$$

Denoting, for the sake of convenience, the transmitted bit sequence to be $\{a_i;\ i = -n_1, \ldots, -1, 0, +1, \ldots, +n_2\}$, the various quantities in eqns. 48–51 can be shown to be given by

$$A_{-1} = \sum_{k=1}^{n_1} C_k^- A_{-1k} \quad (52)$$

$$A_{+1} = \sum_{k=1}^{n_2} C_k^+ A_{+1k} \quad (53)$$

where

$$A_{-1k} = \begin{cases} 1 + \text{sinc}\,(h^{(p)}_{-[k]}\exp\,(-ja^j_{-k}\pi h^{(p)}_{-[k]}), & \text{REC} \\ 1 + J_0(a^j_{-k}\pi h^{(p)}_{-[k]})\exp\,(-ja^j_{-k}\pi h^{(p)}_{-[k]}), & \text{HCS} \\ 1 + p(h^{(p)}_{-[k]}) - ja^j_{-k}R(h^{(p)}_{-[k]}), & \text{RC} \end{cases} \quad (54)$$

$$A_{+1k} = \begin{cases} 1 + \text{sinc}\,(h^{(p)}_{+[k+1]}\exp\,(-ja^j_{+k}\pi h^{(p)}_{+[k+1]}), & \text{REC} \\ 1 + J_0(a^j_{+k}\pi h^{(p)}_{+[k+1]})\exp\,(-ja^j_{+k}\pi h^{(p)}_{+[k+1]}), & \text{HCS} \\ 1 + P(h^{(p)}_{+[k+1]}) - ja^j_{+k}R(h^{(p)}_{+[k+1]}), & \text{RC} \end{cases} \quad (55)$$

and

$$C_k^{\pm} = 0.5\prod_{k-1}^{\pm}\exp\,(-j\theta^{\pm}_{jk}) \quad (56)$$

$$\theta^-_{jk} = \pi\sum_{r=1} a^j_{-r}h^{(p)}_{[r]} \quad (57)$$

$$\theta^+_{jk} = \pi\sum_{r=1}^{k-1} a^j_{+r}h^{(p)}_{+[r+1]} \quad (58)$$

The quantity

$$A_0 = 1, \text{ REC, HCS, RC,} \quad (59)$$

and $B_{\pm 1}$ is related $A_{\pm 1}$ via

$$B_{-1} = A_{-1}, \text{ REC, HCS, RC} \quad (60)$$

and

$$B_{+1} = A_{+1}\exp\,(-j2\pi h^{(p)}_{+[1]}), \text{ REC, HCS, RC} \quad (61)$$

The quantity $B_0$ is given by

$$B_0 = \begin{cases} \text{sinc}\,(h^{(p)}_{+[1]})\exp\,(-j\pi h^{(p)}_{+[1]}), & \text{REC} \\ J_0(\pi h^{(p)}_{+[1]})\exp\,(-j\pi h^{(p)}_{+[1]}), & \text{HCS} \\ P(h^{(p)}_{+[1]}) - jR(h^{(p)}_{+[1]}), & \text{RC} \end{cases} \quad (62)$$

The various quantities in eqn. 50 are given via

$$V_{-1} = \sum_{k=1}^{n_1}[C_k^-]^2 V_{-1k} \quad (63)$$

and

$$V_{+1} = \sum_{k=1}^{n_2}[C_k^+]^2 V_{+1k} \quad (64)$$

where

$$V_{-1k} = \begin{cases} 1 + \text{sinc}\,(2h^{(p)}_{-[k]}), & \text{REC} \\ 1 + \cos\,(\pi h^{(p)}_{-[k]})J_0(\pi h^{(p)}_{-[k]}), & \text{HCS} \\ 1 + P(h^{(p)}_{-[k]}), & \text{RC} \end{cases} \quad (65)$$

and

$$V_{+1k} = \begin{cases} 1 + \text{sinc}\,(2h^{(p)}_{+[k+1]}), & \text{REC} \\ 1 + \cos\,(\pi h^{(p)}_{+[k+1]})J_0(\pi h^{(p)}_{+[k+1]}), & \text{HCS} \\ 1 + P(h^{(p)}_{+[k+1]}), & \text{RC} \end{cases} \quad (66)$$

The relationship between $V_{\pm 1}$ and $R_{\pm 1}$ may be shown to be given by

$$R_{+1} = V_{+1}\exp\,(-j2\pi h^{(p)}_{+[1]}), \text{ REC, HCS, RC} \quad (67)$$

and

$$R_{-1} = V_{-1}, \text{ REC, HCS, RC} \quad (68)$$

The quantity

$$R_0 = B_0 \quad (69)$$

for all three phase functions REC, HCS, and RC.